Kidney International, Vol. 68 (2005), pp. 121–132

Kidneys with heavy proteinuria show fibrosis, inflammation, and oxidative stress, but no tubular phenotypic change

Arvi-Matti Kuusniemi, Risto Lapatto, Christer Holmberg, Riitta Karikoski, Juhani Rapola, and Hannu Jalanko

Hospital for Children and Adolescents and Biomedicum Helsinki, University of Helsinki, Helsinki, Finland

Kidneys with heavy proteinuria show fibrosis, inflammation, and oxidative stress, but no tubular phenotypic change.

Background. Sustained proteinuria is a major factor leading to kidney fibrosis and end-stage renal failure. Tubular epithelial cells are believed to play a crucial role in this process by producing mediators leading to fibrosis and inflammation. Congenital nephrotic syndrome of the Finnish type (NPHS1) is a genetic disease caused by mutations in a podocyte protein nephrin, which leads to constant heavy proteinuria from birth. In this work we studied the tubulointerstitial changes that occur in NPHS1 kidneys during infancy.

Methods. The pathologic lesions and expression of profibrotic and proinflammatory factors in nephrectomized NPHS1 kidneys were studied by immunohistochemistry, Western blotting, and cytokine antibody array. Oxidative stress in kidneys was assessed by measurement of gluthatione redox state.

Results. The results indicated that (*1*) severe tubulointerstitial lesions developed in NPHS1 kidneys during infancy; (*2*) tubular epithelial cells did not show transition into myofibroblasts as studied by the expression of vimentin, α-smooth muscle actin (α-SMA), collagen, and matrix metalloproteinases 2 and 9 (MMP-2 and -9); (*3*) the most abundant chemokines in NPHS1 tissue were neutrophil activating protein-2 (NAP-2), macrophage inhibiting factor (MIF), and monocyte chemoattractant protein-1 (MCP-1); (*4*) monocyte/macrophage cells expressing CD14 antigen were the major inflammatory cells invading the interstitium; (*5*) the arteries and arterioles showed intimal hypertrophy, but the microvasculature in NPHS1 kidneys remained quite normal; and (*6*) excessive oxidative stress was evident in NPHS1 kidneys.

Conclusion. Heavy proteinuria in NPHS1 kidneys was associated with interstitial fibrosis, inflammation, and oxidative stress. The tubular epithelial cells, however, were resistant to proteinuria and did not show epithelial-mesenchymal transition.

Sustained heavy proteinuria is believed to lead to progressive kidney damage [1]. High urinary protein content may elicit proinflammatory and profibrotic effects that contribute to chronic tubulointerstitial damage and loss of renal function [2]. Several in vitro studies have demonstrated that urinary proteins stimulate tubular epithelial cells to secrete factors, such as monocyte chemoattractant protein-1 (MCP-1), that promote inflammation [3]. This is associated with an influx of inflammatory cells to interstitium as well as activation and proliferation of interstitial fibroblasts. The major profibrotic factor implicated in this process is transforming growth factor-β (TGF-β) [4]. Tubular epithelial cells can also directly promote fibrosis by producing extracellular matrix (ECM) components. Tubular epithelial cells may undergo epithelial-mesenchymal transition (EMT) into myofibroblasts, which may invade interstitium [5]. With increased fibrosis and inflammation the number of functioning nephrons progressively declines and renal failure ensues.

The data on the pathophysiologic lesions caused by proteinuria are mainly based on animal models and cell culture studies. In this work we evaluated the tubulointerstitial changes in kidneys with congenital nephrotic syndrome of the Finnish type (CNF, NPHS1). NPHS1 is a recessively inherited renal disease caused by mutations in the nephrin gene [6]. Nephrin is a podocyte-specific protein located at the slit diaphragm of kidney glomerulus. The two most common mutations in the nephrin gene, Fin-major and Fin-minor, lead to a severe disorder characterized by lack of nephrin in the kidney glomerulus and massive proteinuria (up to 100 g/L) starting already during the fetal period [7]. Children with NPHS1 are nephrectomized as infants and their kidneys serve as a unique material for studying the consequences of continuous, heavy proteinuria. Since the basic defect in NPHS1 only affects the glomerular filter, all tubulointerstitial lesions observed are secondary to the protein leakage.

In this work, we used immunohistochemistry, Western blotting, cytokine array, and glutathione analysis to evaluate the nature of the tubulointerstitial lesions, possible changes in tubular epithelial cell phenotype, cortical cytokine production, and oxidative state in NPHS1 kidneys.

Key words: nephrin, proteinuria, tubulointerstitial fibrosis, NAP-2, oxidative stress.

Received for publication December 21, 2004
and in revised form February 1, 2005
Accepted for publication February 11, 2005

METHODS

Tissue samples

A total of 52 kidneys were nephrectomized from children with NPHS1 between 1986 and 2003. The age of the patients at the time of nephrectomy ranged from 4 to 44 months. Before nephrectomy these children were treated with daily albumin infusions to supplement the continuous heavy proteinuria. Routine formalin-fixed paraffin-embedded samples were taken from the kidneys and the rest of the renal cortex was snap-frozen in liquid nitrogen and stored at −70°C.

As controls we used eight normal adult kidneys (age 47 to 58 years) removed for transplantation. These kidneys had proved unsuitable for transplantation mainly because of vascular abnormalities. Formalin-fixed paraffin-embedded sections and snap-frozen samples were collected. The cadaver kidneys had to be used as controls, since fresh tissue samples from normal infant kidneys were not possible to obtain. In the cytokine array, porcine kidney samples were used as additional controls, since brain death may affect the cytokine expression. Porcine kidney samples were obtained from two newborns and one 6-month-old pig. They were snap-frozen and stored at −70°C.

The study protocol was approved by the ethical committee of the Hospital for Children and Adolescents of the University of Helsinki.

Antibodies

The following antibodies were purchased from DakoCytomation (Glostrup, Denmark): CD20cy (M0755), CD68 (M0876), pan-Ig (against IgA, IgG, and IgM) (P0212), α-smooth muscle actin (α-SMA) (M0851), and vimentin (M7020). Antibodies acquired from Santa Cruz Biotechnology (Santa Cruz, CA, USA) were heat shock protein 27 (HSP27) (sc-1048), NAP-2 (sc-19224), pan-cytokeratin (sc-8018), megalin (sc-16476), TGF-β1 (sc-146), HSP27 (sc-1048) and vascular endothelial growth factor (VEGF) (sc-7269). Antibodies against CD3 (ab828), CD14 (ab8679), and collagen type I (ab6308) were bought from Abcam (Cambridge, Cambridgeshire, UK). Anticollagen type VI (MAB3303) was bought from Chemicon International (Temecula, CA, USA), and anti-CD13 (MS-1079-S) and anti-myeloperoxidase (MPO) (RB-373-A) from NeoMarkers (Fremont, CA, USA). In addition we had two anti-MCP-1 antibodies: ALX-804–465 from Alexis Biochemicals (Lausen, Switzerland) and AF-279-NA from R&D Systems (Minneapolis, MN, USA). All these primary antibodies were unconjugated, except for horseradish peroxidase (HRP)-conjugated pan-Ig antibodies, and the dilutions used ranged from 1:10 to 1:250 in immunohistochemistry and from 1:1000 to 1:3000 in Western blotting.

We used the following markers for different cell types: CD13 for monocytes, CD68 for macrophages, CD14 for monocytes and macrophages and some of their subpopulations, MPO for granulocytes and monocytes, CD3 for T lymphocytes, CD20cy for B lymphocytes, mast cell tryptase (MCT) for activated mast cells and pan-immunoglobulin (pan-Ig) antibody for immunoglobulin producing plasma cells.

Light microscopy

The histologic lesions in NPHS1 kidneys were evaluated by light microscopy from paraffin-embedded tissue sections stained with hematoxylin and eosin or periodic acid silver methenamin (PASM). In order to quantitate the changes, interstitial fibrosis, inflammatory cells, tubular cysts, and glomerular sclerosis were graded from 0 to 3. The total histologic score was the sum of these values and ranged from 0 (normal) to 12 (severely damaged). The samples were scored independently by two experienced renal pathologists.

Immunohistochemistry

For the immunofluorescence stainings, the cryosections (5 μm) of the kidney samples were fixed with 3.5% paraformaldehyde or acetone, depending on the antibody used. The stainings were performed in a traditional way. Sections used as negative control were incubated in phosphate-buffered saline (PBS) instead of a primary antibody.

Immunoperoxidase stainings were performed on the sections of formalin-fixed, paraffin-embedded renal samples in a conventional way. To improve antibody penetration, microwave treatment in 10 mmol/L citric acid for 10 minutes was performed or Dako Target Retrieval Solution (S1699) (DakoCytomation) was used depending on the antibody. Amplification of the primary antibody reaction was achieved by incubating the sections with biotinylated secondary antibody (Vector Elite ABC Kit) (Vector Laboratories Inc., Burlingame, CA, USA). Immunoperoxidase staining of cryosections was performed similarly. The sections were fixed with 3.5% paraformaldehyde or acetone depending on the antibody used.

Light microscopy was performed with a standard Leica DM RX light microscope equipped with an Olympus DP70 digital camera. To calculate the area fraction of a particular immunostained component images were imported to the freeware image analysis program NIH ImageJ 1.32j (National Institutes of Health, Bethesda, MD, USA). Sequential gray-scale images were grabbed using the ×10 objective. The presence of glomeruli in the fields was ignored and a threshold was applied to each image at a constant level that distinguished between the stained component and the background. The proportion of black

to white pixels in the image was then calculated as a percentage [8].

All immunohistochemical data presented were analyzed from at least four control and six NPHS1 kidneys.

Western blotting

Tissue samples of kidney cortex were homogenized with Ultra-Turrax (Rose Scientific Ltd., Alberta, Canada) in Laemmli sample buffer, and the proteins were separated on a gel (8% to 12%) and blotted onto an Immobilon-P polyvinylidene fluoride (PVDF) membrane (Millipore, Billerica, MA, USA). After blocking with 5% nonfat dry milk in PBS, the membrane was stained with a primary antibody followed by a peroxidase-conjugated secondary antibody (Jackson ImmunoResearch, West Grove, PA, USA). Bound antibodies were visualized using enhanced chemiluminescence (ECL) (Amersham Biosciences, Uppsala, Sweden).

Cytokine array

Custom human cytokine antibody array (RayBiotech Inc., Atlanta, GA, USA) consisted of 50 different cytokine and chemokine antibodies spotted in duplicate onto a membrane [9]. The experiments were performed according to manufacturer's instructions. Briefly, tissue samples of kidney cortex were homogenized in lysis buffer, centrifuged at 14,000 rpm for 10 minutes. The protein concentration was measured using DC Protein Assay (Bio-Rad, Hercules, CA, USA). Membranes were incubated with blocking buffer, 500 μg of tissue lysate was added to the membrane and incubated over night at 4°C. After washes, membranes were incubated with biotinylated antibody for 2 hours, washed, and incubated for 1 hour with HRP-conjugated streptavidin. Unbound reagents were washed, and the membranes were developed with the ECL system (Amersham Biosciences). Chemiluminescence was quantified with Scion Image Beta 4.02 Win analysis software. The results were expressed as relative signal intensities so that positive control spots included in each membrane were given an intensity value of 100.

Terminal deoxynucleotidyl transferase (TdT)-mediated deoxyuridine triphosphate (dUTP) nick end labeling (TUNEL)

The occurrence of apoptosis in kidney tubules was analyzed by monitoring the presence of DNA fragmentation [10]. Slides were analyzed by conventional light microscopy after light counterstaining with hematoxylin. Cells exhibiting dark brown staining from the colorimetric reaction were considered positive for DNA fragmentation. Negative controls, conducted by omitting the labeling enzyme, yielded no reaction product. As positive controls we used testis samples with abundant apoptosis.

Glutathione analysis

The oxidative stress in the kidney cortex was evaluated by the measuring the total and free glutathione levels as previously described [11]. In brief, free sulfhydryls of thiols were derivatized with monobromobimane to form fluorescent complexes. Thiols were then separated with high-performance liquid chromatography (HPLC) and detected fluorometrically. This gives the concentration of free thiols. In order to measure the total (reduced + oxidized) concentration of glutathione, samples of renal cortex were first treated with dithiothreitol to reduce disulphides.

Statistics

Data are presented as mean ± standard deviation (SD). Statistical analyses were carried out using the Student t test. Two-tailed P values < 0.05 were considered significant.

RESULTS

The histology of the 52 NPHS1 kidneys nephrectomized at the age of 4 to 44 months ranged from nearly normal to severely damaged (Fig. 1A and B). The findings included glomerulosclerosis, interstitial fibrosis and inflammation, arterial wall thickening, tubular atrophy and dilatation, and accumulation of proteinaceous material into tubular lumen. There was a considerable variation in the rate of progression of the renal lesions during the first year as shown by the histologic scoring (Fig. 1C).

Tubular epithelial cell phenotype

Tubular cells contained protein and lipid rich vesicles as studied by high magnification (Fig. 2A). Dilatation of tubules with flattening of epithelial cells was quite common. Tubular basement membrane ruptures in PASM staining were seen in 0.4% and 0.5% of the well-preserved tubuli in NPHS1 and control kidneys, respectively (Table 1) (Fig. 2B to D). Tubular atrophy with widened tubular basement membrane was often first detected in the vicinity of glomeruli and sharp borders between the degenerating and healthy tubular profiles were typically seen (Fig. 2F). The number of apoptotic tubular cells detected by TUNEL was similar in NPHS1 and control kidneys (0.04% and 0.06%) (P = NS) (Table 1). The number of Ki-67–positive proliferating tubular cells was fourfold in NPHS1 kidneys (0.2% of tubular cells) as compared to controls (0.05%) ($P = 0.07$) (Table 1). The number of tubular epithelial cells with condensed nucleus (apoptosis/mitosis) were 4.4 and 5.5 per 100 tubules

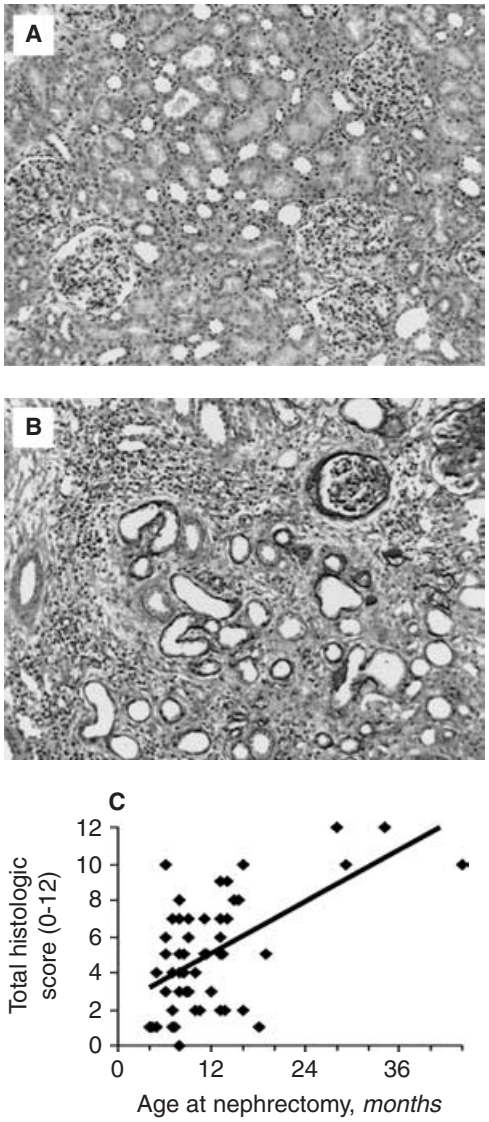

Fig. 1. Progression of renal damage in NPHS1 kidneys. The histology of 52 NPHS1 kidneys ranged from nearly normal to severely damaged. (*A*) NPHS1 kidney nephrectomized at 4 months showing normal histology. (*B*) Severe lesions are seen in NPHS1 kidneys nephrectomized at the age of 28 months. Glomerulosclerosis, inflammation, tubular dilatation, and tubulointerstitial fibrosis have evolved. (*C*) The relationship between renal damage and age at nephrectomy was studied from kidney samples of 52 NPHS1 patients that were scored based on tubular cysts, interstitial fibrosis, inflammatory cells, and sclerosed glomeruli. The rate of progression of damage varies considerably among NPHS1 kidneys ($R^2 = 0.34$) [(A and B) periodic acid silver methanamin (PASM) staining].

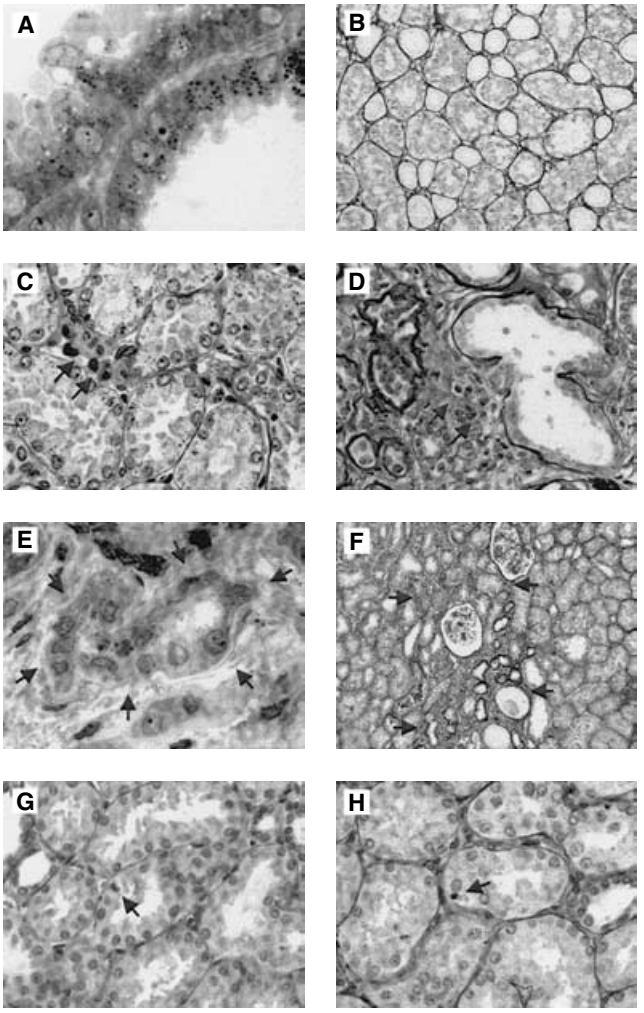

Fig. 2. Photomicrographs of tubules in NPHS1 patients. (*A*) Close view of the walls of two adjacent tubules showing accumulation of proteinaceous material (black) and occasional lipid droplets (white) inside tubular epithelial cells. (*B*) Silver staining showing intact tubular basement membranes in tubuli. (*C* and *D*) Ruptures of the tubular basement membrane were very rare and usually associated with interstitial fibrosis and accumulation of mononuclear inflammatory cells (arrows). (*E*) In areas of severe lesions, atrophied tubules were a common finding (encircled by arrows). (*F*) Tubular atrophy and interstitial fibrosis were first evident in periglomerular areas and showed a clear-cut change (arrows) to normal-looking cortical areas. (*G*) Condensed nuclei speaking for apoptosis or mitosis of tubular epithelial cells (arrow) were present. (*H*) Inflammatory cells were infrequent inside tubules (arrow) and tubulitis was therefore not a characteristic feature of NPHS1 kidneys [periodic acid silver methanamin (PASM) stainings].

in NPHS1 and control kidneys, respectively (P = NS) (Fig. 2G) (Table 1).

The expression of tubular epithelial cell proteins megalin (Fig. 3A to C) and cytokeratin (Figs. 3D to F and 4A) were comparable in control and NPHS1 kidneys with normal histology (Table 1). Vimentin-positive tubular cells were present in relatively high numbers, more in NPHS1 than control kidneys ($P < 0.005$) (Table 1) (Fig. 3I). By contrast, only four possibly α-SMA–positive tubular cells were found in 651 visual fields (approximately 117,000 tubular epithelial cells) (Fig. 3L) (Table 1). Similarly, tubular epithelium did not express type I collagen (Fig. 3O) (Table 1). Immunofluorescence staining for matrix metalloproteinases 2 and 9 (MMP-2 and -9) revealed positive cells in interstitium and glomeruli but very few tubular cells stained for these enzymes (Fig. 5A and B) (Table 1).

Table 1. Characteristics of tubular epithelial cells in NPHS1 and control kidneys

Tubular findings	NPHS1	Control
	Area fraction%[a]	
Megalin		
Minor changes	4.5% ± 3.2%	4.6% ± 2.2%
Severe lesions	2.3% ± 1.3%	—
Cytokeratin		
Minor changes	16.2% ± 7.1%	21.8% ± 5.2%
Severe lesions	15.8% ± 10.4%	—
	Positive cells/100 tubular cross-sections[b]	
Tubular basement membrane ruptures		
Normal morphology	0.37 (2/531)	0.53 (3/570)
Fibrotic interstitium	2.78 (13/468)	—
Tubular epithelial cells with condensed nucleus		
Normal morphology	2.75 (11/400)	5.5 (11/200)
Fibrotic interstitium	6 (12/200)	—
Invading inflammatory cells		
Normal morphology	9.03 (27/299)	2.6 (15/577)
Fibrotic interstitium	12.72 (92/723)	—
TUNEL	0.48 (69/14400)	0.73 (44/6000)
Ki-67	2.46 (207/8400)	0.69 (25/3600)
α-smooth muscle actin	0.05 (5/8775)	0 (0/990)
Vimentin	127.1 (4920/3870)	40.3 (2000/4965)
Collagen type I	0.08 (5/5940)	0.17 (8/4620)
Matrix metalloproteinase 2	0.26 (6/2325)	0.13 (3/2400)
Matrix metalloproteinase 9	0.4 (14/4500)	0.32 (9/2850)
Transforming growth factor-β	0 (0/4500)	0.37 (11/7300)

TUNEL is terminal deoxynucleotidyl transferase (TdT)-mediated deoxyuridine triphosphate (dUTP) nick end labeling.
[a]Area fraction results are expressed as mean ± SD of at least four control and at least nine (four minor + five severe lesions) NPHS1 kidneys.
[b]Tubular findings were calculated from at least four control and six NPHS1 kidneys. In parenthesis; number of positive findings/number of tubular cross-sections analyzed.

Small clusters and solitary cytokeratin-positive cells were present in the fibrotic interstitium in NPHS1 kidneys (Fig. 3F). None of these cells, however, stained for α-SMA or type I collagen, as studied by double immunoperoxidase stainings (500 visual fields analyzed; data not shown).

Interstitial fibrosis and peritubular capillaries

Interstitial fibrosis was first evident in the vicinity of glomeruli and sclerotic arteries as well as around degenerating tubuli (Fig. 6A and B). Due to fibrosis the peritubular space became progressively wider. Immunoperoxidase staining and Western blotting showed increased amounts of collagen type I and type VI, vimentin, and α-SMA in NPHS1 kidneys as compared controls (Figs. 3G to O and 4B to E). Thickening of arterial and arteriolar walls was evident in NPHS1 kidneys (Fig. 6A and B). However, the peritubular capillary endothelial surface area was intact as suggested by immunoperoxidase staining for the endothelial cell marker CD34 (Fig. 6C to E). Even so, the peritubular capillary lumen size was diminished by 47% (Fig. 6F).

Inflammatory cells

Inflammatory cell clusters first appeared in the vicinity of degenerating glomeruli in NPHS1 kidneys (Fig. 7A). The amount of peritubular inflammatory cells was less pronounced, and it was variable in the fibrotic areas surrounding the degenerating tubuli. The interstitial inflammatory cells in the peritubular area were mainly of the monocyte/macrophage lineage in NPHS1 kidneys (Fig. 7). The most abundant cells amidst tubuli were CD14-positive monocyte/macrophages (Fig. 7C and G). CD3-positive T lymphocytes were the second largest group of cells in NPHS1 kidneys (Fig. 7D and G). Interestingly, tubulitis was not evident (Fig. 2H). Proximal and distal tubules of NPHS1 and control kidneys contained comparable numbers of mononuclear cells (Table 1).

Cytokines and chemokines

The tissue content of 50 cytokines, chemokines, and some growth factors in the kidney cortex was analyzed by the cytokine antibody array (Fig. 8). The most significant finding was that the signal for neutrophil activating peptide 2 (NAP-2) in NPHS1 kidneys was 46 times and 14 times stronger than in pig and human controls, respectively. Also, the levels of two monocytic chemokines, MCP-1 (4.2×), and MIF (3.6×) were clearly elevated. Other molecules, whose levels in NPHS1 kidney were clearly elevated as compared to normal pig kidneys, were angiogenin (10× as compared to pig tissue), intercellular adhesion molecule-1 (ICAM-1) (4.6×), interleukin (IL)-1 receptor antagonist (IL-1ra) (3.3×) tumor necrosis

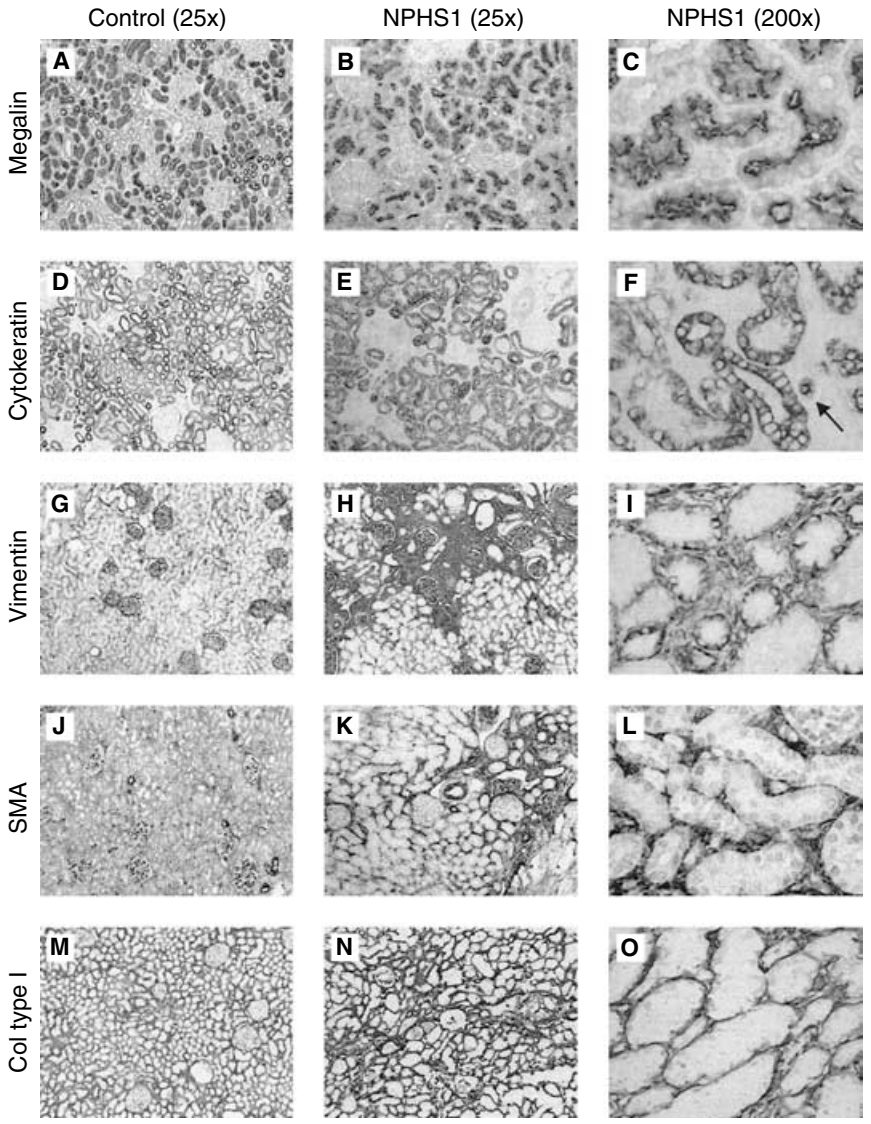

Fig. 3. Immunoperoxidase staining of tubular epithelial cell phenotype markers in NPHS1 kidneys. (*A* to *C*) Tubular epithelial cell membrane receptor megalin was expressed in the same manner and quantity in NPHS1kidneys with mild changes as in controls. (*D* to *F*) The same holds true for the epithelial cell marker cytokeratin. Small clusters of cytokeratin-positive cells were present in the fibrotic interstitium [arrow in (F)]. (*G*) Mesenchymal marker vimentin was expressed only in glomerular podocytes in control kidneys. (*H*) Increased vimentin positivity was seen in NPHS1 kidney interstitium. (*I*) Many of the tubular epithelial cells expressed vimentin in NPHS1 kidneys. (*J*) α-smooth muscle actin (α-SMA) expression was limited to mesangial cells and blood vessel smooth muscle cells in control kidneys. (*K*) In the areas of cortical matrix, the expression of α-SMA was increased in NPHS1 kidneys. (*L*) There were no tubular epithelial cells positive for α-SMA. (*M* and *N*) Increased fibrosis was present throughout NPHS1 kidneys as seen by collagen type I staining. (*O*) There were no collagen type I expressing tubular epithelial cells.

factor-α (TNF-α) (3×), epidermal growth factor (EGF) (2.3×), and regulated upon activation, normal T-cell expressed and secreted (RANTES) (2×).

In immunofluorescence staining the monocytic chemokine MCP-1 and mono- and lymphocytic cytokine MIF were mostly detected in interstitial cells and less so in tubular epithelium (Fig. 5G and H) (Table 1). Immunofluorescence staining of neutrophilic chemokine NAP-2 also showed staining in interstitial cells, but, in addition to this, part of the tubular epithelium expressed NAP-2 in NPHS1 kidneys (Fig. 5E and F).

The tissue content of the major profibrotic factor, TGF-β1, was surprisingly low in the cytokine array and did not significantly differ in NPHS1 and control kidneys (Fig. 8B). Similarly, the immunoperoxidase staining of TGF-β revealed no staining of tubuli and a scattered staining of interstitial cells in NPHS1 kidneys (Table 1). NPHS1 kidneys contained significantly more VEGF in the cytokine array compared to controls. The pattern of immunofluorescence staining was similar to that in control kidneys (Figs. 6G and H and 8B).

Oxidative stress

The interstitium of NPHS1 kidneys contained numerous MPO-positive foci, as analyzed by immunohistochemistry (Fig. 5D). This prompted us to study the total amount of oxidative stress in NPHS1 kidneys. As shown in Figure 9, the concentration of free glutathione was extremely low in NPHS1 kidney cortex as compared to controls ($P < 0.0005$) indicating severe oxidative stress. This

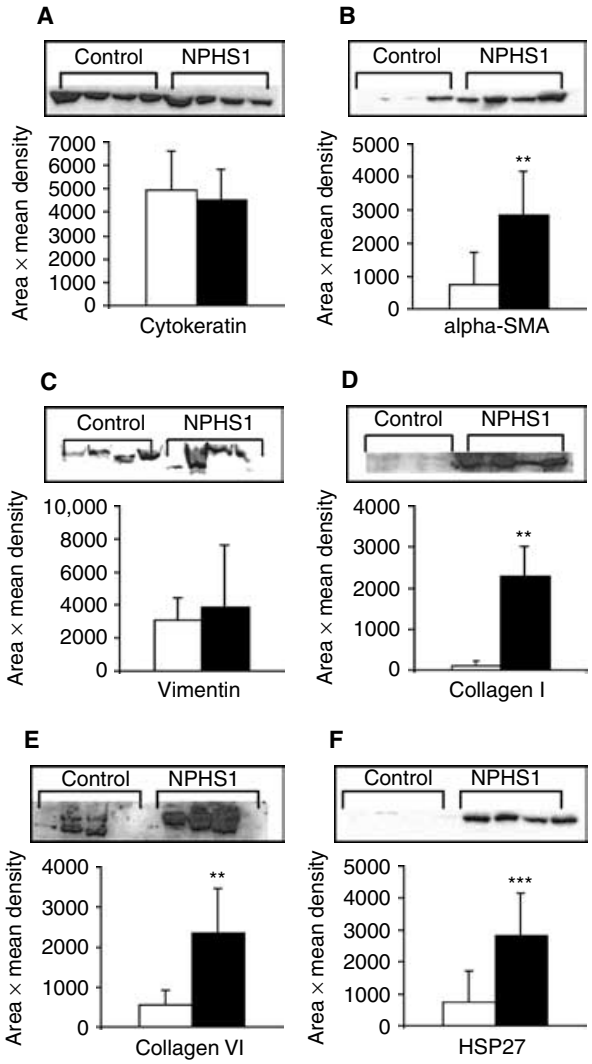

Fig. 4. Western blotting of renal cortex. There was no statistically significant difference in cytokeratin (*A*) or vimentin (*C*) content between NPHS1 (■) and control (□) kidneys. α-smooth muscle actin (α-SMA) (*B*), heat shock protein 27 (HSP27) (*F*), and collagen type I (*D*) and VI (*E*) were significantly more abundant in NPHS1 kidney cortex than in controls. Results are expressed as mean ± SD of two independent experiments with samples of four controls and four NPHS1 kidney cortex. $^{**}P < 0.005$; $^{***}P < 0.0005$.

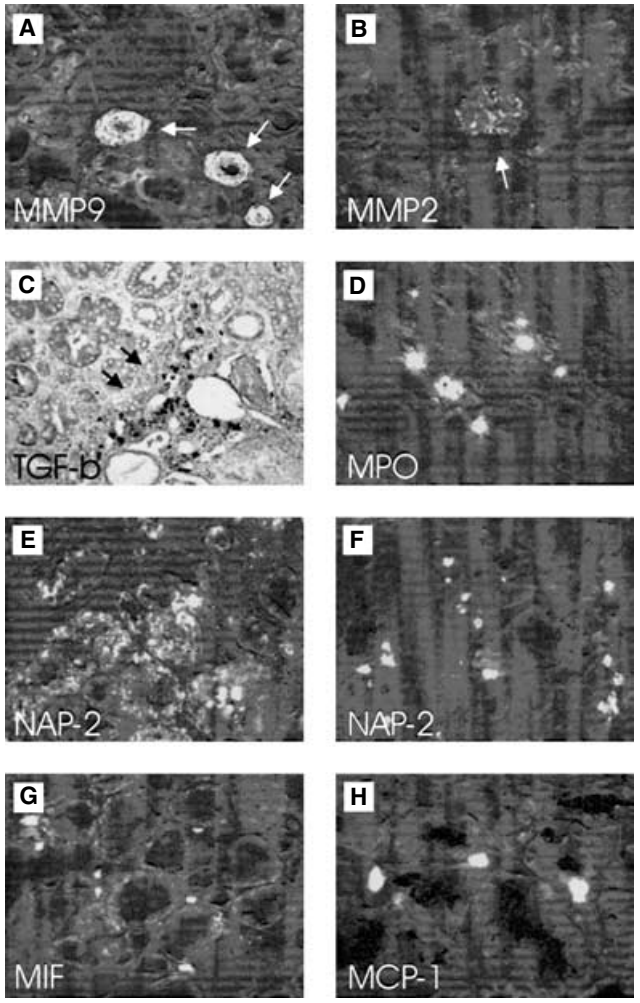

Fig. 5. Immunohistochemical stainings of some of most interesting soluble factors in NPHS1 kidneys. (*A*) Matrix metalloproteinase 9 (MMP-9) was expressed strongly in arterial walls (arrows) of NPHS1 kidneys. (*B*) A faint staining of MMP-2 was seen in the glomeruli (arrow) of NPHS1 kidneys. Neither of the MMPs were expressed in tubular epithelial cells. (*C*) Transforming growth factor-β (TGF-β) staining was strong in interstitial cells (arrows), and no staining was observed in tubules. (*D*) Myeloperoxidase (MPO) was abundant in the interstitium of NPHS1 kidneys. (*E*) Neutrophil activating protein-2 (NAP-2) staining was strong in part of the tubules and (*F*) inflammatory cells. (*G* and *H)* Macrophage inhibiting factor (MIF) and monocyte chemoattractant protein-1 (MCP-1) staining was also seen in inflammatory cells, but there was no tubular staining [immunofluorescence stainings except (C) immunoperoxidase].

was supported by the finding of high levels of HSP27 in NPHS1 kidneys as studied by Western blotting (Fig. 4F).

DISCUSSION

We evaluated the tubulointerstitial changes in human NPHS1 kidneys nephrectomized in the early childhood. Infiltration of the interstitium by monocytic inflammatory cells, oxidative stress, and interstitial fibrosis seemed to be crucial for the progression of the pathologic lesions in the NPHS1 kidneys. On the other hand, changes in the peritubular capillaries or phenotypic transition of the tubular epithelium did not seem to play a role in this process.

Large amounts of plasma proteins leak into tubular lumen and form a heavy burden for the tubular cells in NPHS1 kidneys. Accordingly, the proximal tubular epithelial cells were filled with protein and lipid-rich vesicles. The tubular epithelium, however, seemed to be quite resistant to proteinuria. The rate of apoptosis of tubular epithelial cells was low, and the proliferative response was modest, as evaluated by the number of mitotic cells

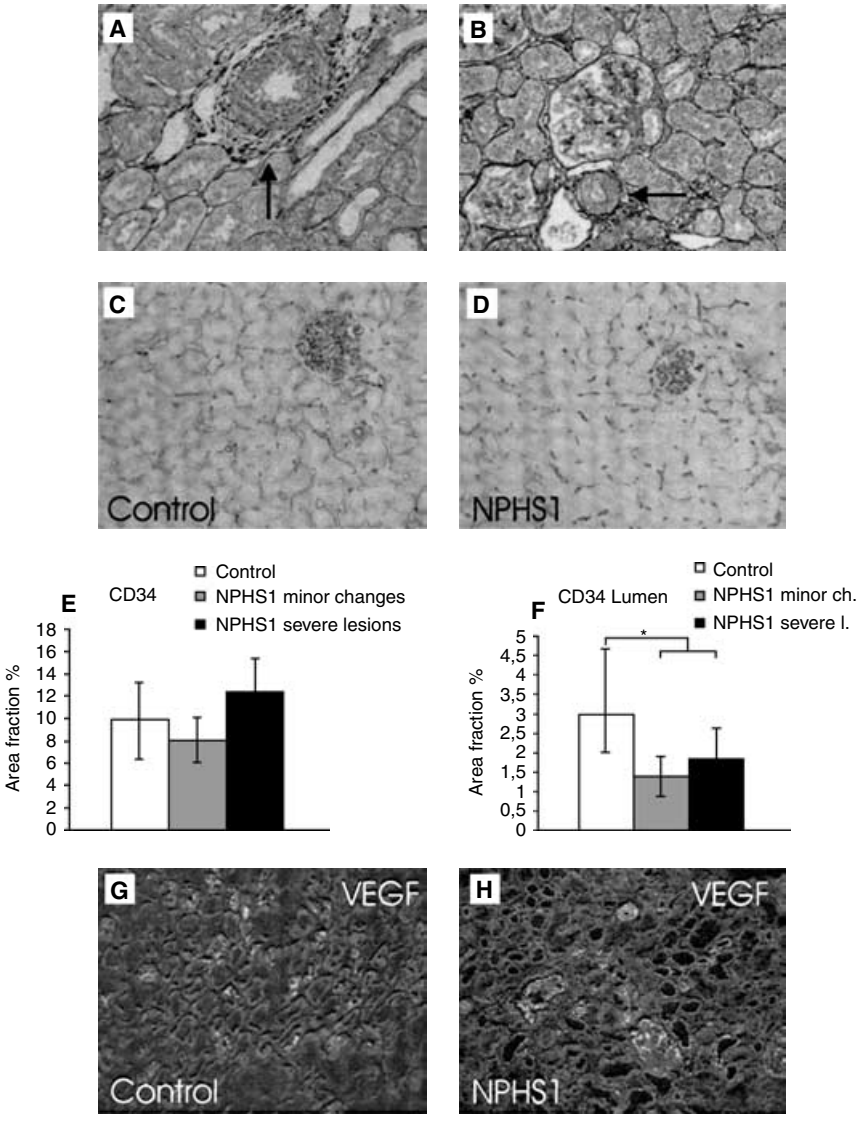

Fig. 6. Renal vasculature in NPHS1 kidneys. (*A*) Arterial wall thickening (arrow) is an early and prominent feature in NPHS1 kidneys and is often accompanied by increased interstitial matrix formation. (*B*) Also the arterioles (arrow) are affected as seen here in the vascular pole of a histologically normal glomerulus. (*C* and *D*) Endothelial marker CD34 was used to analyze changes in renal microvasculature. (*E*) The area fraction% of CD34 immunoperoxidase staining was similar in NPHS1 and control kidneys, but (*F*) the area fraction of vascular lumens was decreased in NPHS1 kidneys compared to controls. Area fractions were measured from five controls and nine NPHS1 kidneys. (*G* and *H*) Vascular endothelial growth factor (VEGF) immunofluorescence staining showed that the expression of VEGF in NPHS1 kidneys was comparable to controls. $^{*}P < 0.05$; [(A and B); periodic acid silver methanamin (PASM) staining].

and the expression of Ki-67. Also, no tubulitis was observed suggesting that urinary proteins did not elicit antigenic stimulus. The expression of cytokeratin and megalin, which is an important receptor for urinary proteins in proximal tubular cells [12], was comparable to control kidneys**.** These structural findings are supported by the previous observations that the tubular function in NPHS1 children remain amazingly normal even after months of massive proteinuria [13, 14]. The NPHS1 children do not have glucosuria or other signs of proximal tubular defect.

EMT of tubular cells has recently been regarded important for the progression of renal fibrosis in animal models [15–17], cell culture works [18–20], and in some human studies [21–23]. Tubular cells with EMT typically express α-SMA, actin filaments, vimentin, type I collagen, fibroblast-specific protein 1 (in mice), and loose epithelial cell markers such as E-cadherin. Some of the transformed cells migrate into peritubular interstitium [15] and produce interstitial matrix components [17]. Up to 30% of the interstitial myofibroblasts have been reported to originate from tubular epithelial cells [17]. This migration requires focal destruction of the tubular basement membrane which is believed to be accomplished by the proteolytic enzymes MMP-2 and MMP-9 secreted by the tubular epithelial cells [5].

We found that a small proportion of the tubular cells in NPHS1 kidneys expressed vimentin which is in agreement with the findings of Rastaldi et al [21], who found tubular vimentin in biopsy samples from various human renal diseases. On the other hand, we found practically no tubular cells positive for α-SMA, type I collagen, MMP2, or MMP9. Also, no cells coexpressing cytokeratin and α-SMA or type I collagen were detected in the interstitium. The findings were based on the analysis of hundreds

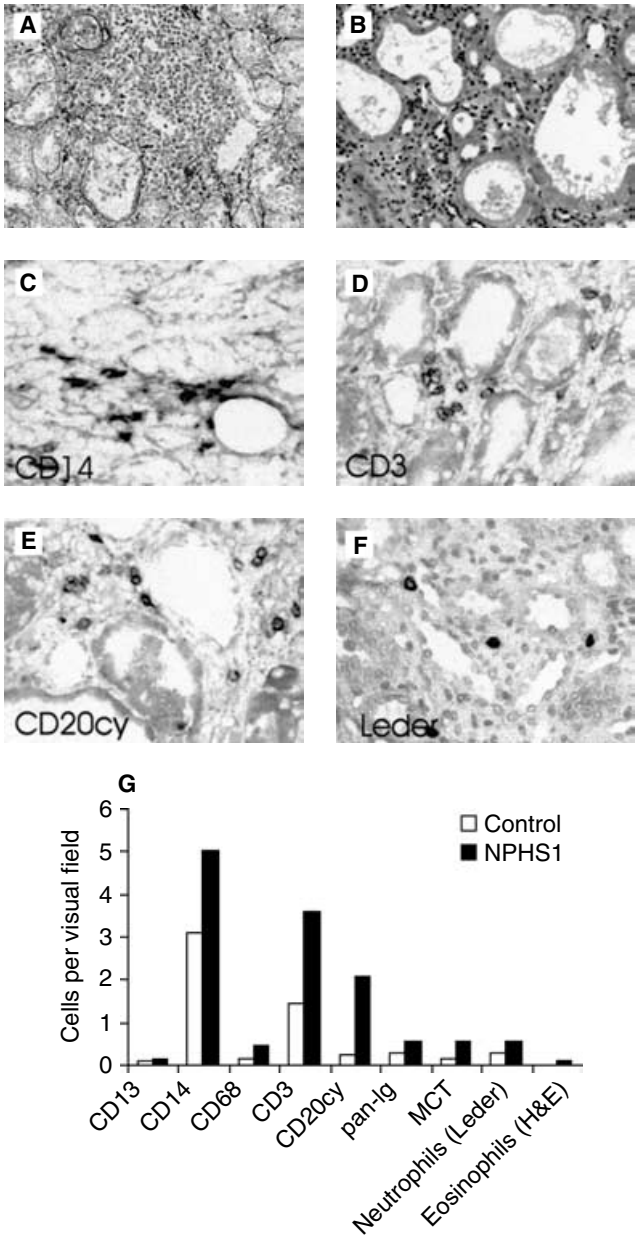

Fig. 7. Light microscopy and immunoperoxidase staining of inflammatory cells in the tubulointerstitium of NPHS1 and control kidneys. (*A* to *F*) NPHS1 kidneys. (A) Inflammatory cell infiltration first appeared in the vicinity of degenerating glomeruli. (B) Solitary and small clusters of inflammatory cells were also evident in the interstitium. The most abundant inflammatory cells in the NPHS1 kidney interstitium were (C) monocytes, (D) T lymphocytes, (E) B lymphocytes, and (F) neutrophils. (*G*) Graph showing positive interstitial cells per visual field. Positive cells from at least 50 visual fields (200×) were counted from each of the seven NPHS1 and four control kidneys. Cells located among tubuli were calculated. Large infiltrates located at periglomerular or totally damaged areas were excluded from these calculations [(A and B) periodic acid silver methanamin (PASM) staining].

of visual fields and strongly suggest that tubular cells in NPHS1 kidneys do not undergo EMT. Since kidneys from young individuals show the highest plasticity, one would expect to detect EMT especially in infant kidneys with proteinuria.

Several cytokines and growth factors are known to promote EMT. TGF-β1 is reported to be able to complete the entire EMT process in vitro [24, 25]. A surprising finding in this study was that NPHS1 kidneys had the same levels of TGF-β1 as human and pig control kidneys in the cytokine array. The immunohistochemical staining revealed few scattered TGF-β1–positive cells in the interstitium but not in the tubular epithelium. Interestingly, the level of hepatocyte growth factor (HGF), which negatively modulates EMT [26], was decreased in NPHS1 kidneys.

Chemokines are believed to play an important role in renal fibrosis by attracting inflammatory cells into the interstitium. Tubular epithelial cells possibly produce chemokines in the early phase [27, 28], but later on they may originate from the infiltrating inflammatory cells [29–31]. MCP-1 is regarded as the most important chemokine in this context. It attracts leukocytes and is involved in the initiation and progression of tubulointerstitial damage [32, 33]. Another interesting chemokine with similar effects is MIF [34]. In NPHS1 kidneys, the tissue levels of both chemokines were clearly elevated but there were no tubular cell staining in immunofluorescence. Surprisingly, very high level of NAP-2 were present in NPHS1 kidneys, and immunofluorescence revealed NAP-2 expression both in tubular and interstitial cells. NAP-2 is one of the β-thromboglobulin (β-TG) proteins produced by many cell types. It preferentially attracts neutrophils and stimulates lysosomal enzyme degranulation in these cells [35], but its role in renal diseases is so far unknown.

Monocyte/magrophages and T lymphocytes were the most abundant inflammatory cells in NPHS1 kidneys. This is in agreement with the result obtained in mice [36] and also in human kidneys [37, 38]. The role of macrophages in chronic renal failure has been emphasized. They may secrete fibrosis-promoting growth factors (e.g., TGF-β) and vasoactive products (e.g., endothelin-1, angiotensin II) and participate in the recruitment of the matrix-producing interstitial myofibroblasts [39].

The loss of peritubular microvasculature and subsequent ischemia has also been reported to play a major role in tubulointerstitial scarring [40]. In NPHS1 kidneys the peritubular capillaries looked narrower than in the control kidneys, but no decrease of the capillary endothelium was seen in the CD34 staining. Also, the endothelial survival factor VEGF was abundantly expressed in the tubulointerstitium of NPHS1 kidneys, as shown by the cytokine array and immunohistochemistry. Thus, loss of peritubular capillaries clearly does no explain the fibrotic process.

The interstitial expression of MPO was strong in the NPHS1 kidneys. This enzyme was mainly produced and secreted by monocyte/macrophages as shown by the double immunofluorescence stainings and reported

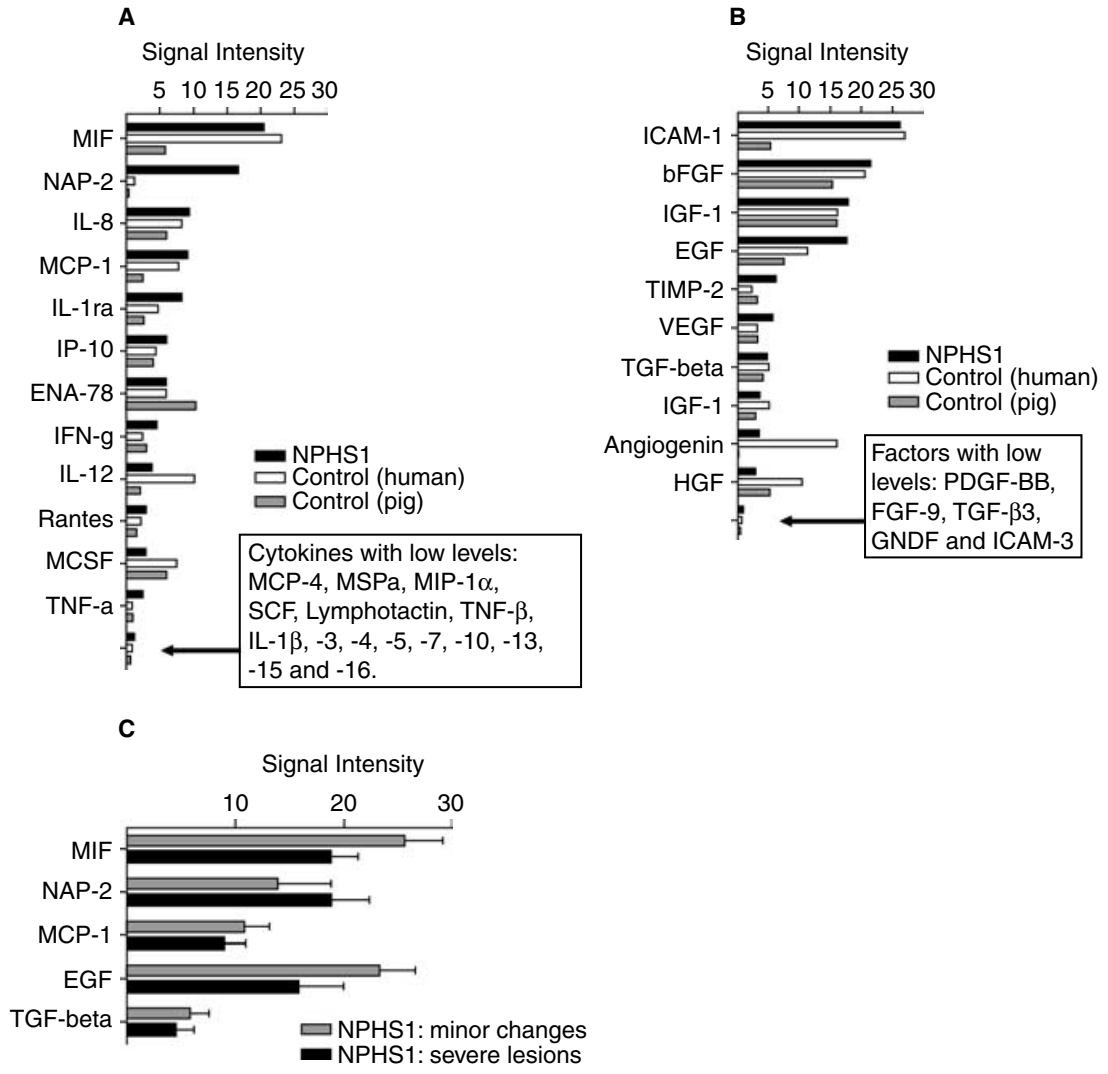

Fig. 8. Antibody array analysis of cytokines, chemokines, and other mediators in NPHS1 kidney cortex. The most abundant mediators are shown as bars and the ones with levels near the detection limit of the array are only mentioned in the box. (*A*) Cytokines. Note the extremely high amount of neutrophil activating protein-2 (NAP-2) in NPHS1 kidneys compared to controls. Also the levels of macrophage inhibiting factor (MIF), monocyte chemoattractant protein-1 (MCP-1), interleukin-1 receptor antagonist (IL-1ra), regulated upon activation, normal T-cell expressed and secreted (RANTES), and tumor necrosis factor-α (TNF-α) were higher in NPHS1 than in controls. (*B*) Growth factors and other mediators. Intercellular adhesion molecule-1 (ICAM-1), epidermal growth factor (EGF), vascular endothelial growth factor (VEGF), and angiogenin levels were higher in NPHS1 kidneys compared to controls. The levels of the major profibrotic factor transforming growth factor-β (TGF-β) were not elevated in NPHS1 kidneys. Hepatocyte growth factor (HGF) levels were lower in NPHS1 kidneys than in controls. (*C*) The most interesting cytokines and growth factors in NPHS1 kidneys divided to two groups based on histologic score. Results are expressed as mean of 10 NPHS1, seven control human and three control pig kidney cortex samples in (A) and (B). In (C) the results are expressed as mean ± SD of four NPHS1 kidneys with minor and of six kidneys with severe lesions.

previously in human diseases [41]. MPO generates a powerful oxidant, hypoclorous acid (HOCl), which may cause permanent tissue damage [42]. The importance of MPO and other possible oxidants was supported by the finding of very low levels of free glutathione in the cortex of NPHS1 kidneys. Glutathione is a major antioxidant in human tissues and the amount of free glutathione decreases in the presence of HOCl and other reactive oxygen species [42]. The high levels of the scaffold protein HSP27 also support the idea that NPHS1 kidneys are under heavy oxidative stress [43].

CONCLUSION

The results in this work suggest that the tubular epithelium is quite resistant to proteinuria. We did not find diffuse tubular atrophy, which would have been caused by the direct toxicity of luminal proteins. Instead, tubular atrophy was associated with interstitial fibrosis and inflammation, which often was periglomerular and segmental at first. Thus, the deleterious effect of proteinuria seems to be indirect and mediated by the peritubular fibrotic and inflammatory process.

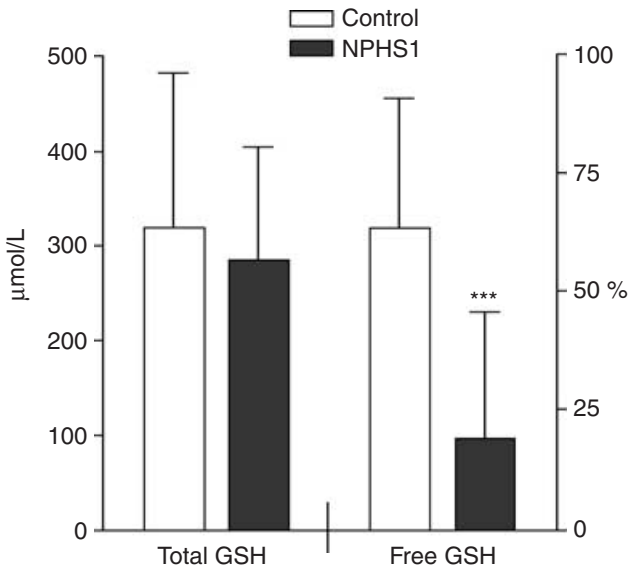

Fig. 9. Total and free glutathione (GSH) levels in NPHS1 and control kidney cortex. Total glutathione levels were nearly equal, but the levels of free glutathione were dramatically reduced in NPHS1 kidneys compared to controls. Samples of 13 NPHS1 and 10 control kidney cortex were tested. Results are expressed as mean ± SD. $^{***}P < 0.0005$ vs. control group.

ACKNOWLEDGMENTS

This work was supported by grants from the Finnish Academy, the Sigrid Juselius Foundation, Pediatric Research Foundation, The Paulo Foundation, and Helsinki University Central Hospital Research Fund. We thank Tuike Helmiö, Taija Havulinna, and Tuija Heinonen for excellent technical assistance.

Reprint requests to Hannu Jalanko, Hospital for Children and Adolescents, University of Helsinki, 00290 Helsinki, Finland.
E-mail: hannu.jalanko@hus.fi

REFERENCES

1. Ruggenenti P, Remuzzi G: The role of protein traffic in the progression of renal diseases. *Annu Rev Med* 51:315–327, 2000
2. Zoja C, Benigni A, Remuzzi G: Cellular responses to protein overload: Key event in renal disease progression. *Curr Opin Nephrol Hypertens* 13:31–37, 2004
3. Anders HJ, Vielhauer V, Schlondorff D: Chemokines and chemokine receptors are involved in the resolution or progression of renal disease. *Kidney Int* 63:401–415, 2003
4. Bottinger EP, Bitzer M: TGF-beta signaling in renal disease. *J Am Soc Nephrol* 13:2600–2610, 2002
5. Liu Y: Epithelial to mesenchymal transition in renal fibrogenesis: Pathologic significance, molecular mechanism, and therapeutic intervention. *J Am Soc Nephrol* 15:1–12, 2004
6. Kestila M, Lenkkeri U, Mannikko M, *et al*: Positionally cloned gene for a novel glomerular protein–nephrin–is mutated in congenital nephrotic syndrome. *Mol Cell* 1:575–582, 1998
7. Patrakka J, Kestila M, Wartiovaara J, *et al*: Congenital nephrotic syndrome (NPHS1): Features resulting from different mutations in Finnish patients. *Kidney Int* 58:972–980, 2000
8. Furness PN: The use of digital images in pathology. *J Pathol* 183:253–263, 1997
9. Lin Y, Huang R, Chen LP, *et al*: Profiling of cytokine expression by biotin-labeled-based protein arrays. *Proteomics* 3:1750–1757, 2003
10. Tilly JL: Use of the terminal transferase DNA labeling reaction for the biochemical and in situ analysis of apoptosis, in *Cell Biology: A Laboratory Handbook* (vol. 1), edited by Celis JE, San Diego, Academic Press, 1994, pp 330–337
11. Ahola T, Fellman V, Laaksonen R, *et al*: Pharmacokinetics of intravenous N-acetylcysteine in pre-term new-born infants. *Eur J Clin Pharmacol* 55:645–650, 1999
12. Verroust PJ, Birn H, Nielsen R, *et al*: The tandem endocytic receptors megalin and cubilin are important proteins in renal pathology. *Kidney Int* 62:745–756, 2002
13. Patrakka J, Kestila M, Wartiovaara J, *et al*: Congenital nephrotic syndrome (NPHS1): Features resulting from different mutations in Finnish patients. *Kidney Int* 58:972–980, 2000
14. Antikainen M, Holmberg C, Taskinen MR: Growth, serum lipoproteins and apoproteins in infants with congenital nephrosis. *Clin Nephrol* 38:254–263, 1992
15. Ng YY, Huang TP, Yang WC, *et al*: Tubular epithelial-myofibroblast transdifferentiation in progressive tubulointerstitial fibrosis in 5/6 nephrectomized rats. *Kidney Int* 54:864–876, 1998
16. Yang SP, Woolf AS, Quinn F, Winyard PJ: Deregulation of renal transforming growth factor-beta1 after experimental short-term ureteric obstruction in fetal sheep. *Am J Pathol* 159:109–117, 2001
17. Iwano M, Plieth D, Danoff TM, *et al*: Evidence that fibroblasts derive from epithelium during tissue fibrosis. *J Clin Invest* 110:341–350, 2002
18. Strutz F, Okada H, Lo CW, *et al*: Identification and characterization of a fibroblast marker: FSP1. *J Cell Biol* 130:393–405, 1995
19. Oldfield MD, Bach LA, Forbes JM, *et al*: Advanced glycation end products cause epithelial-myofibroblast transdifferentiation via the receptor for advanced glycation end products (RAGE). *J Clin Invest* 108:1853–1863, 2001
20. Li Y, Yang J, Dai C, *et al*: Role for integrin-linked kinase in mediating tubular epithelial to mesenchymal transition and renal interstitial fibrogenesis. *J Clin Invest* 112:503–516, 2003
21. Rastaldi MP, Ferrario F, Giardino L, *et al*: Epithelial-mesenchymal transition of tubular epithelial cells in human renal biopsies. *Kidney Int* 62:137–146, 2002
22. Jinde K, Nikolic-Paterson DJ, Huang XR, *et al*: Tubular phenotypic change in progressive tubulointerstitial fibrosis in human glomerulonephritis. *Am J Kidney Dis* 38:761–769, 2001
23. Nadasdy T, Laszik Z, Blick KE, *et al*: Tubular atrophy in the end-stage kidney: A lectin and immunohistochemical study. *Hum Pathol* 25:22–28, 1994
24. Yang J, Liu Y: Dissection of key events in tubular epithelial to myofibroblast transition and its implications in renal interstitial fibrosis. *Am J Pathol* 159:1465–1475, 2001
25. Fan JM, Ng YY, Hill PA, *et al*: Transforming growth factor-beta regulates tubular epithelial-myofibroblast transdifferentiation in vitro. *Kidney Int* 56:1455–1467, 1999
26. Yang J, Liu Y: Blockage of tubular epithelial to myofibroblast transition by hepatocyte growth factor prevents renal interstitial fibrosis. *J Am Soc Nephrol* 13:96–107, 2002
27. Wang Y, Rangan GK, Tay YC, *et al*: Induction of monocyte chemoattractant protein-1 by albumin is mediated by nuclear factor kappaB in proximal tubule cells. *J Am Soc Nephrol* 10:1204–1213, 1999
28. Zoja C, Donadelli R, Colleoni S, *et al*: Protein overload stimulates RANTES production by proximal tubular cells depending on NF-kappa B activation. *Kidney Int* 53:1608–1615, 1998
29. Furuichi K, Wada T, Sakai N, *et al*: Distinct expression of CCR1 and CCR5 in glomerular and interstitial lesions of human glomerular diseases. *Am J Nephrol* 20:291–299, 2000
30. Ou ZL, Natori Y, Natori Y: Gene expression of CC chemokines in experimental acute tubulointerstitial nephritis. *J Lab Clin Med* 133:41–47, 1999
31. Schadde E, Kretzler M, Banas B, *et al*: Expression of chemokines and their receptors in nephrotoxic serum nephritis. *Nephrol Dial Transplant* 15:1046–1053, 2000
32. Tesch GH, Schwarting A, Kinoshita K, *et al*: Monocyte chemoattractant protein-1 promotes macrophage-mediated tubular injury, but not glomerular injury, in nephrotoxic serum nephritis. *J Clin Invest* 103:73–80, 1999
33. Wada T, Furuichi K, Sakai N, *et al*: Up-regulation of monocyte chemoattractant protein-1 in tubulointerstitial lesions of human diabetic nephropathy. *Kidney Int* 58:1492–1499, 2000

34. Lan HY, Yang N, Nikolic-Paterson DJ, *et al*: Expression of macrophage migration inhibitory factor in human glomerulonephritis. *Kidney Int* 57:499–509, 2000
35. Brandt E, Ludwig A, Petersen F, Flad HD: Platelet-derived CXC chemokines: Old players in new games. *Immunol Rev* 177:204–216, 2000
36. Eddy AA: Interstitial nephritis induced by protein-overload proteinuria. *Am J Pathol* 135:719–733, 1989
37. Hooke DH, Gee DC, Atkins RC: Leukocyte analysis using monoclonal antibodies in human glomerulonephritis. *Kidney Int* 31:964–972, 1987
38. Nikolic-Paterson DJ, Hurst L, Atkins RC: Macrophages in immune renal injury, in *Immunologic Renal Disease* (2nd ed.), edited by Neilson EG, Couser WG, Philadelphia, Lippincott, Williams & Wilkins, 2001, pp 609–632
39. Chai Q, Krag S, Chai S, *et al*: Localisation and phenotypical characterisation of collagen-producing cells in TGF-beta 1-induced renal interstitial fibrosis. *Histochem Cell Biol* 119:267–280, 2003
40. Kang DH, Kanellis J, Hugo C, *et al*: Role of the microvascular endothelium in proggressive renal disease. *J Am Soc Nephrol* 13:806–816, 2002
41. Malle E, Buch T, Grone HJ: Myeloperoxidase in kidney disease. *Kidney Int* 64:1956–1967, 2003
42. Pullar JM, Winterbourn CC, Vissers MC: Loss of GSH and thiol enzymes in endothelial cells exposed to sublethal concentrations of hypochlorous acid. *Am J Physiol* 277:1505–1512, 1999
43. Arrigo AP: Hsp27: Novel regulator of intracellular redox state. *IUBMB Life* 52:303–307, 2001